Acid Sulfate Soils Research Program

Lower Lakes Hydro-Geochemical Model Development and Assessment of Acidification Risks

Report 6 | Part 3 of 4 | October 2010

Australian Government

Government of South Australia

WATER FOR GOOD

7   Scenario analysis

Following on from the model validation process, various scenarios were run in the model using the same model configurations and parameters, but with extended inflow and meteorological forcing data. The major aim was to assess the acidification risks that could be posed by continued water level decline in the Lower Lakes, and in particular how the dynamics of stabilisation scenarios compared to a continued drawdown, 'do nothing' scenario.

7.1   Lake Albert: drawdown scenarios and analysis (Sep 2009 – Sep 2013)

Lake Albert water quality forecast

The validation simulations above highlight the importance of evapo-concentration and calcite solubility control for accurately capturing the geochemical dynamics of Lake Albert from 2008-2009. In order to explore the potential futures states of the lake, '*yPP*' configured simulations (i.e. solubility control enabled for $CaCO_3$, MnO_2, $FeOH_3$, $AlOH_3$) were run to Jan 2013 with the acid sulfate soil module, using the configuration and parameters from the Currency/Finniss domain validation presented in the previous chapter, without alteration. Results from the scenarios are shown in Figures 7.1–7.10. Several scenarios of pumping of water from Lake Alexandrina were simulated including a post-2009 withdrawal of pumping (i.e., 'do nothing'), and stabilisation at various levels, as outlined in the Table 7.1. Meteorological data from Narrung weather station, Hindmarsh Valley and Pelican Pt was repeated from the 2009 record year to year for the forecast years.

The water level results (Figure 7.1) from the model indicate that if pumping is not maintained throughout 2010, then the lake will dry to below -1.5m by Apr 2011. Additional pumping in the -1.0m scenario maintains this level until Summer 2011-2012, when the lake begins to drop quickly, and much of the sediment becomes exposed (as indicated by the flat lines at the non-central locations). Stabilisation is achieved slightly above the target(s) for the -0.75m and -0.50m AHD pumping scenarios.

The corresponding salinity plot for the scenarios indicates a rapid increase above 30,000 uScm^{-1} during early 2010, but this is diluted by winter rains. It rapidly increases again over summer and into 2011 to around 50,000 uScm^{-1} (i.e., around seawater) should pumping not continue. Note that this model may underestimate the salinity and the dilution process in this case since salt left in dry cells is not re-dissolved upon rewetting. The scenarios indicate that the salinity will remain around 25,000 uScm^{-1} in the lake centre if stabilisation occurs at around -0.75m or -0.5m, assuming there is no substantial change in Lake Alexandrina salinity over this period.

The DIC and pH plots (Figure 7.2) highlight the rapid decrease in pH and carbonate alkalinity in Dec 2010 if pumping is discontinued. For the scenario where the water level is maintained at -1.0m, the alkalinity remains high until Jan 2012 when the water level drops in the hot, dry conditions. The alkalinity (and pH) is maintained in both of the stabilisation scenarios at -0.75m and -0.5m. The other ions follow similar trends as salinity as is expected. The dissolved metals Al, Mn and FeIII (FeIII not shown) in the acidifying scenarios show that they reach very high levels following the onset of acidification due to dissolution from the mineral phases (Figure 7.6-7.7).

The total nutrients reach very high levels in all scenarios due to evapo-concentration (Figure 7.8-7.10) and this may lead to deteriorating water quality given the depth will also be low. Oxygen remains fairly constant from year to year, but the DOC accumulates significantly as the water level drops (Figure 7.8). The total Chlorophyll-a concentration also remains above 100 ugL^{-1} for much of the year post 2010 (Figure 7.9).
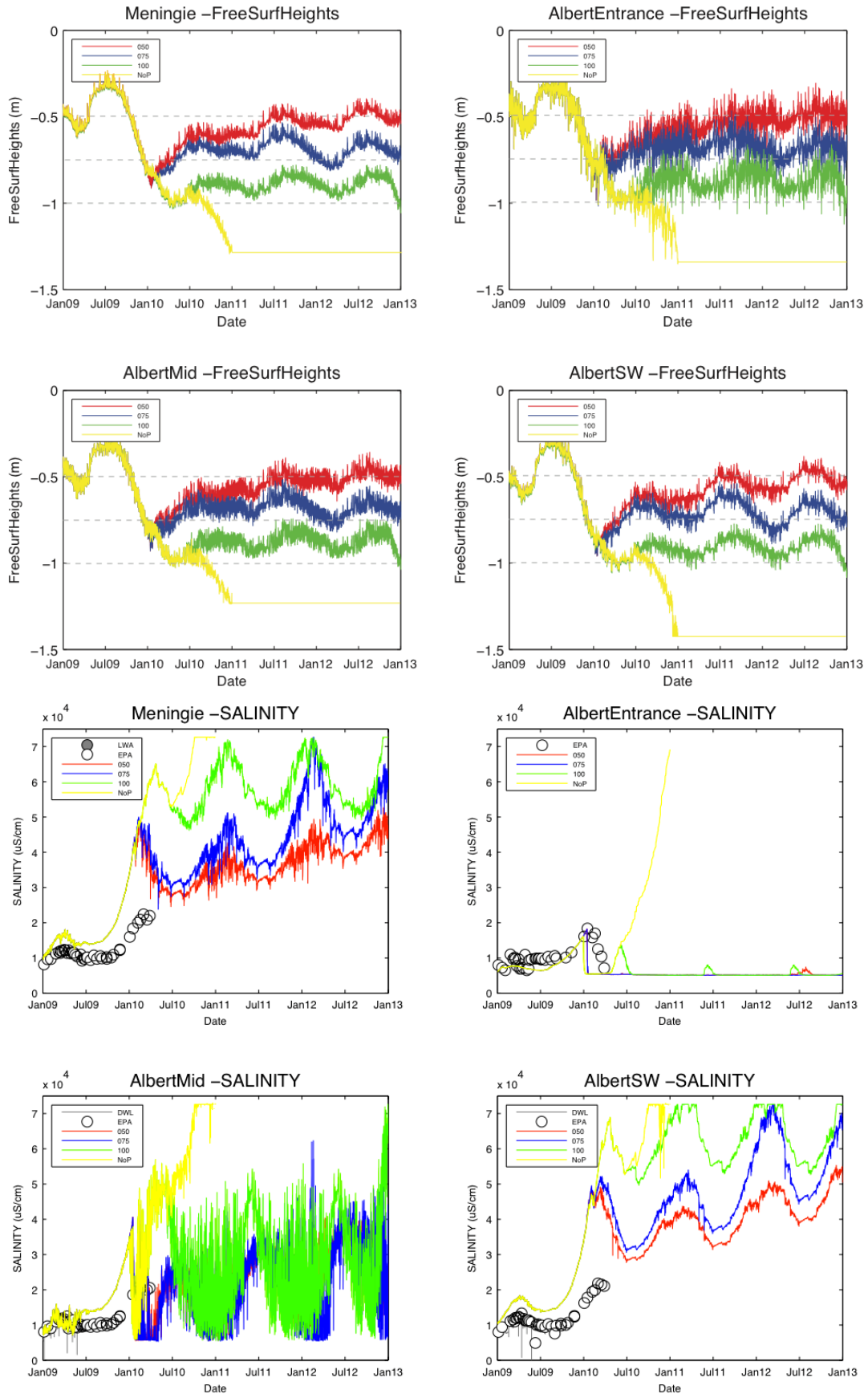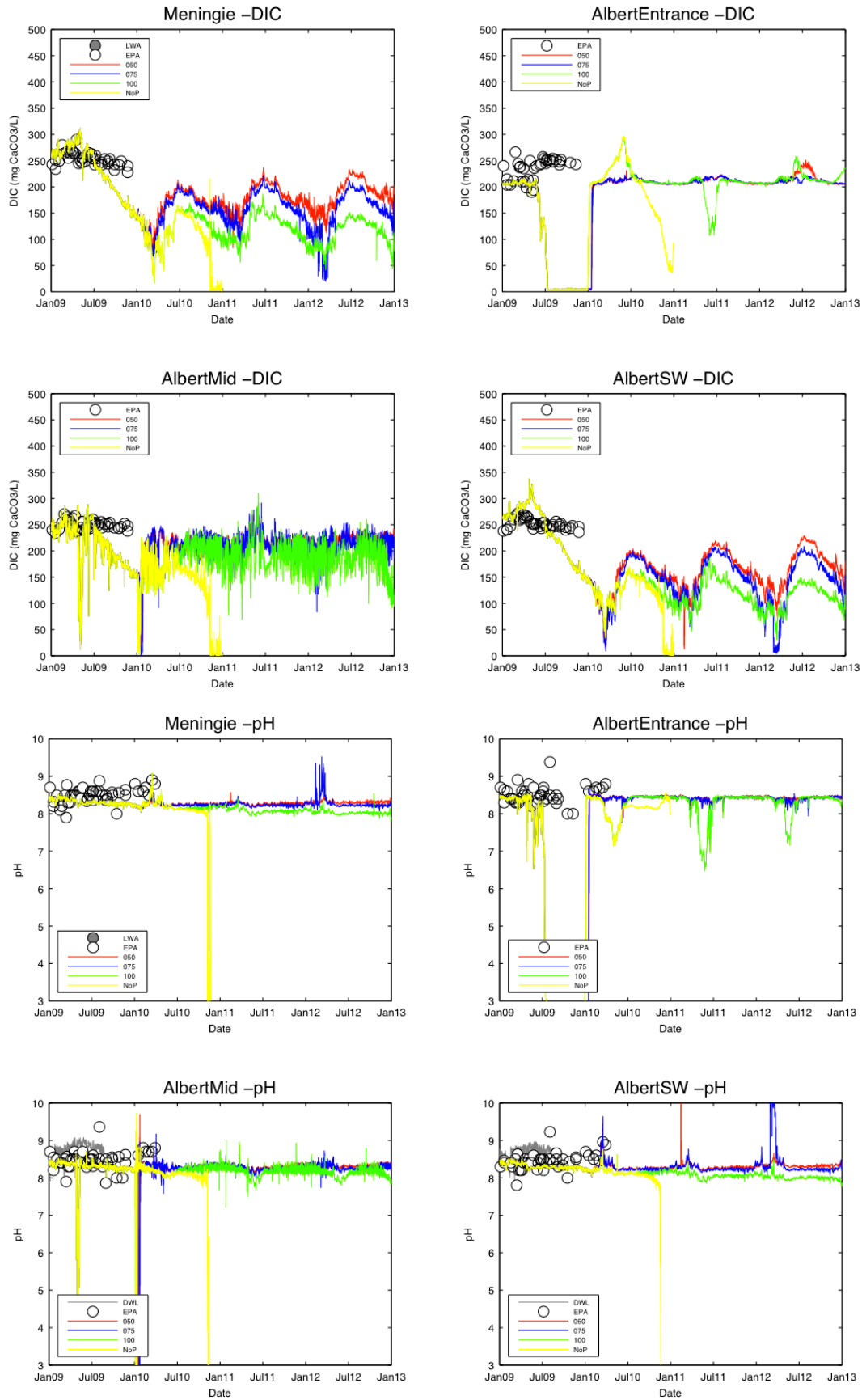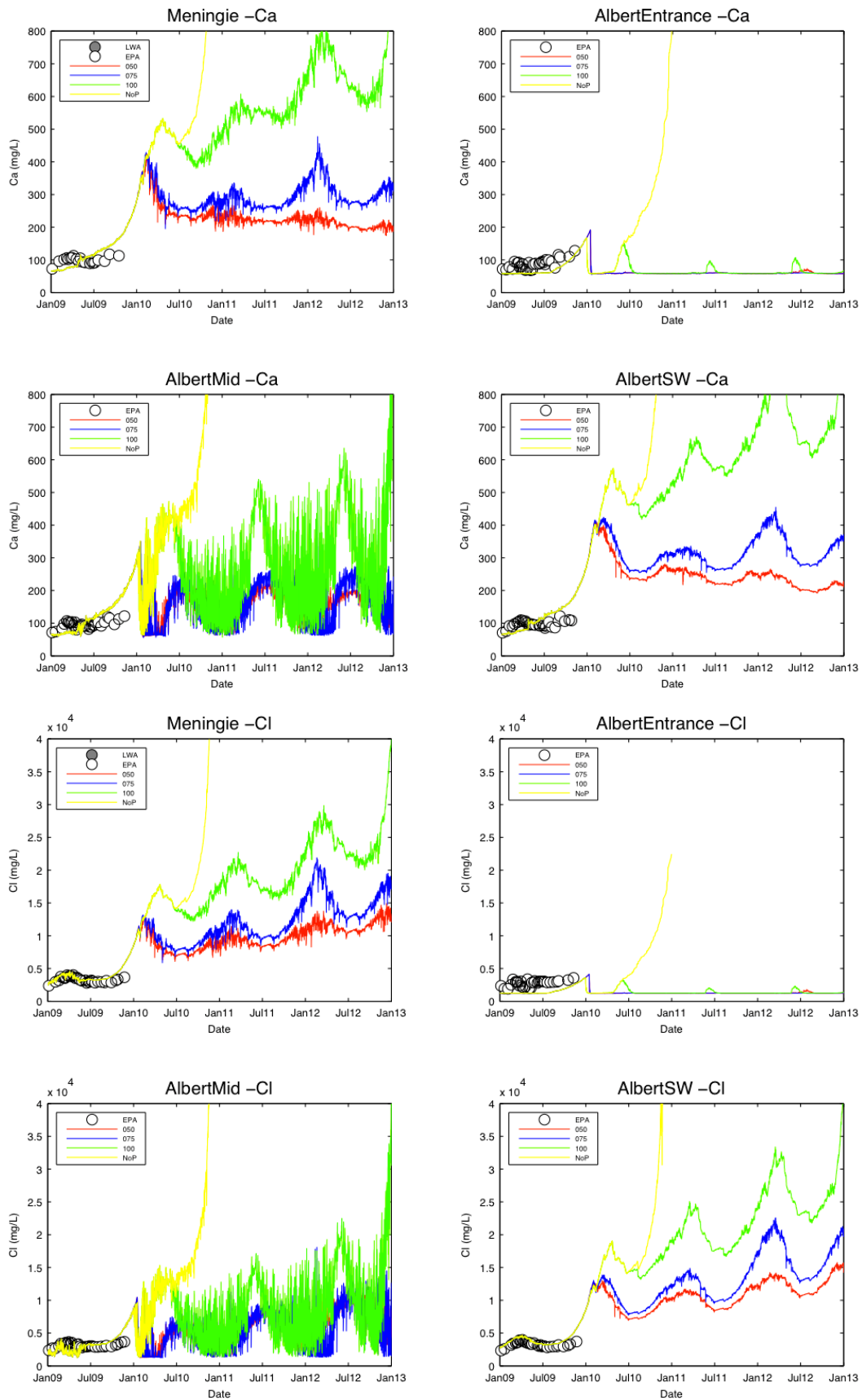
Figure 7.1: Forecast scenarios of modelled (NoP: no continued pumping; 100: stabilisation at -1.0m AHD; 075: stabilisation at -0.75m AHD; 050: stabilisation at -0.5m AHD) water level (mAHD) and salinity (as expressed by conductivity, uS cm⁻¹) for four stations within Lake Albert.
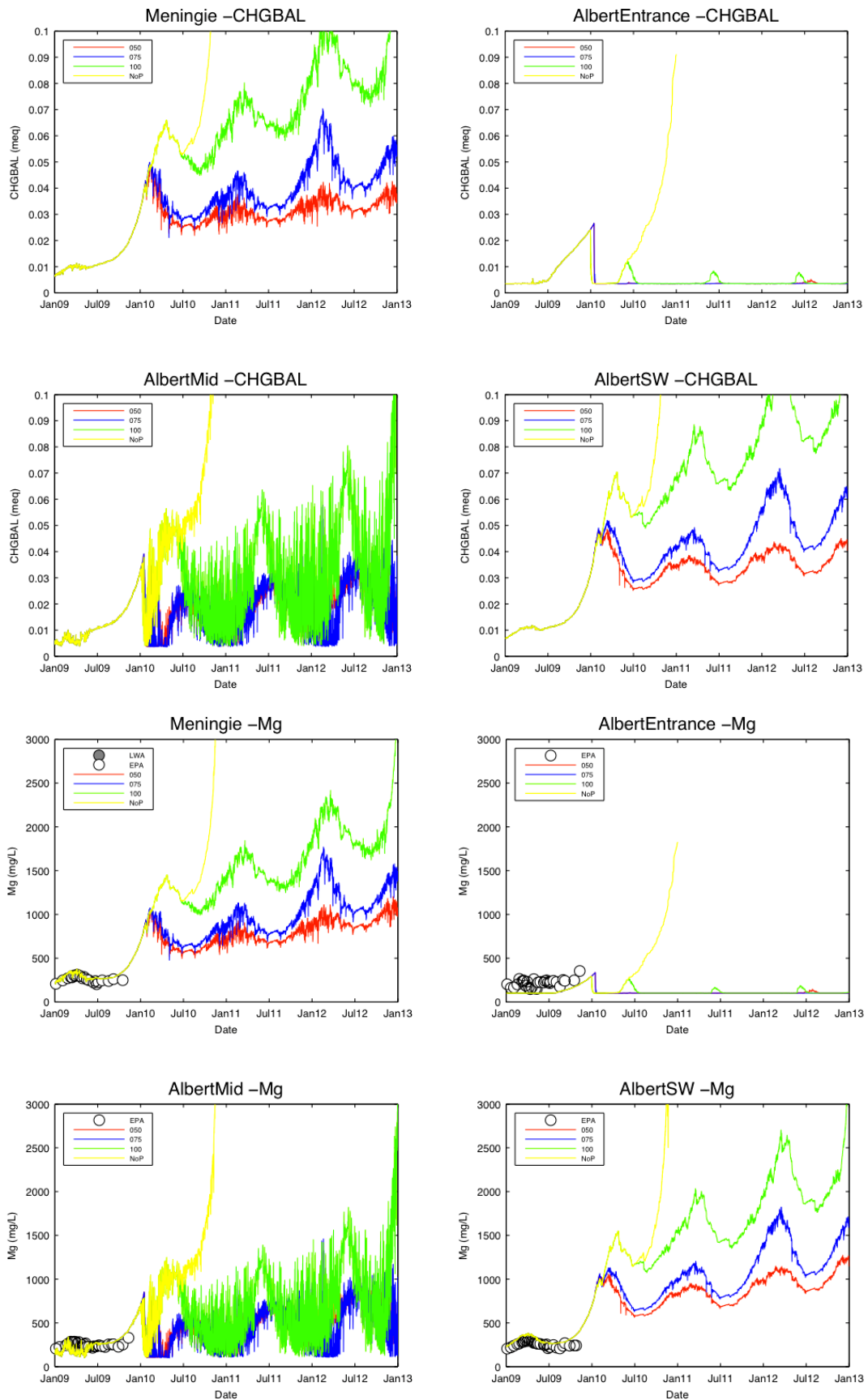
Figure 7.2: Forecast scenarios of modelled (NoP: no continued pumping; 100: stabilisation at -1.0m AHD; 075: stabilisation at -0.75m AHD; 050: stabilisation at -0.5m AHD) dissolved carbonate alkalinity (DIC, as mg CaCO$_3$ L^{-1}) and pH (-) for four stations within Lake Albert.
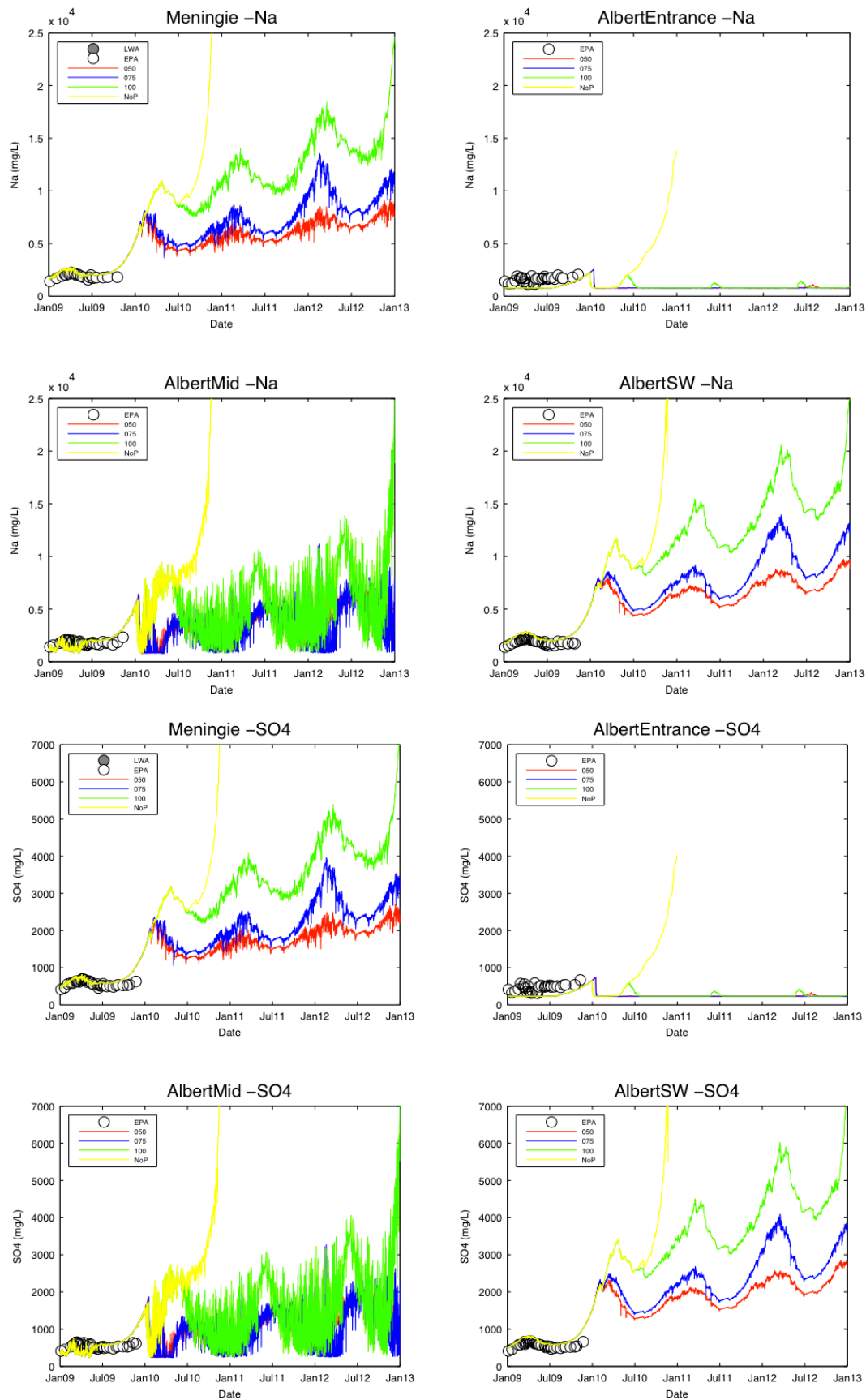
Figure 7.3: Forecast scenarios of modelled (NoP: no continued pumping; 100: stabilisation at -1.0m AHD; 075: stabilisation at -0.75m AHD; 050: stabilisation at -0.5m AHD) Ca (mg L⁻¹) and Cl (mg L⁻¹) for four stations within Lake Albert.
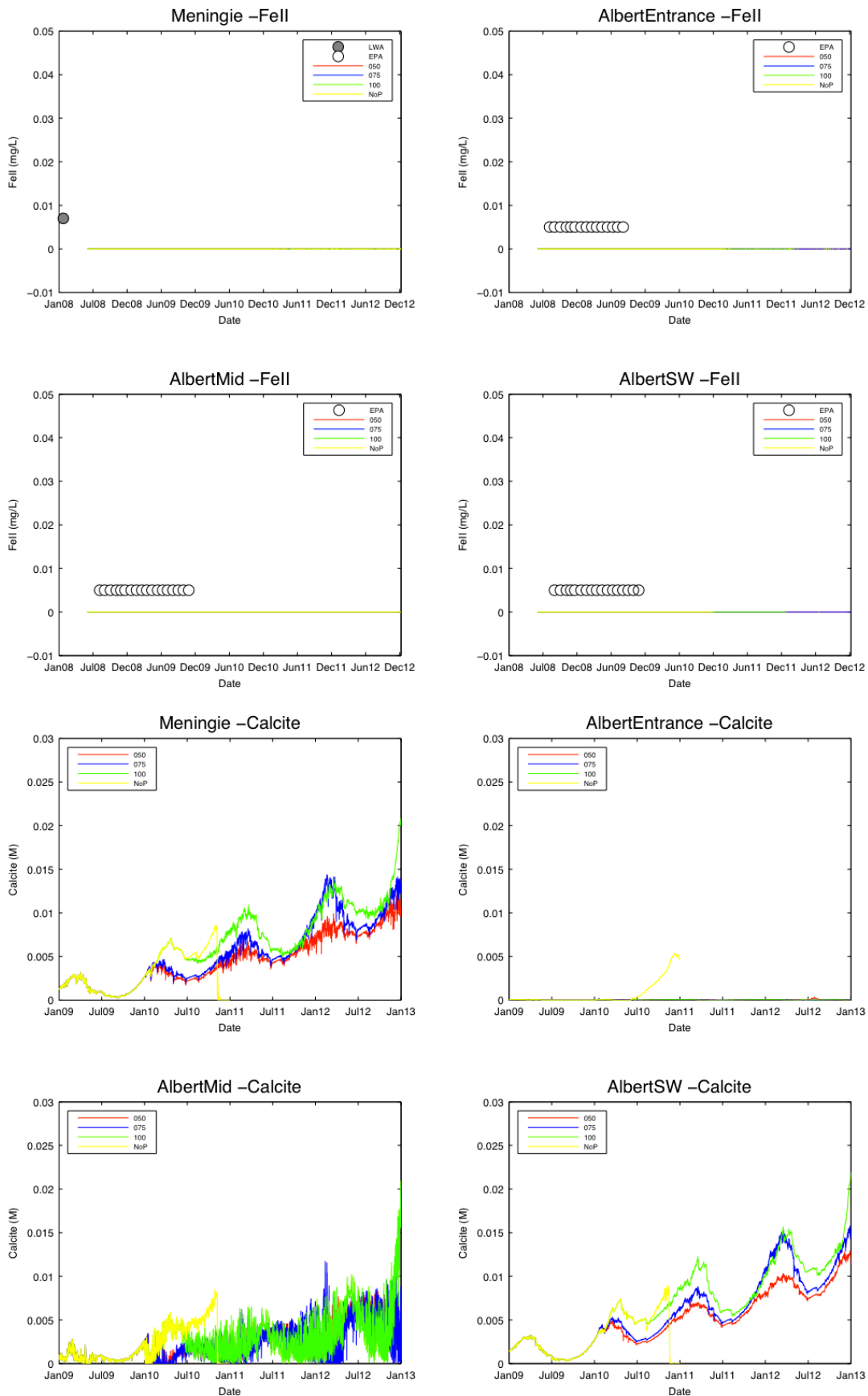
Figure 7.4: Forecast scenarios of modelled (NoP: no continued pumping; 100: stabilisation at -1.0m AHD; 075: stabilisation at -0.75m AHD; 050: stabilisation at -0.5m AHD) charge imbalance (CHGBAL (meq) and Mg (mg L^{-1}) for four stations within Lake Albert.

Figure 7.5: Forecast scenarios of modelled (NoP: no continued pumping; 100: stabilisation at -1.0m AHD; 075: stabilisation at -0.75m AHD; 050: stabilisation at -0.5m AHD) Na (mg L-1) and SO4 (mg L-1) for four stations within Lake Albert.
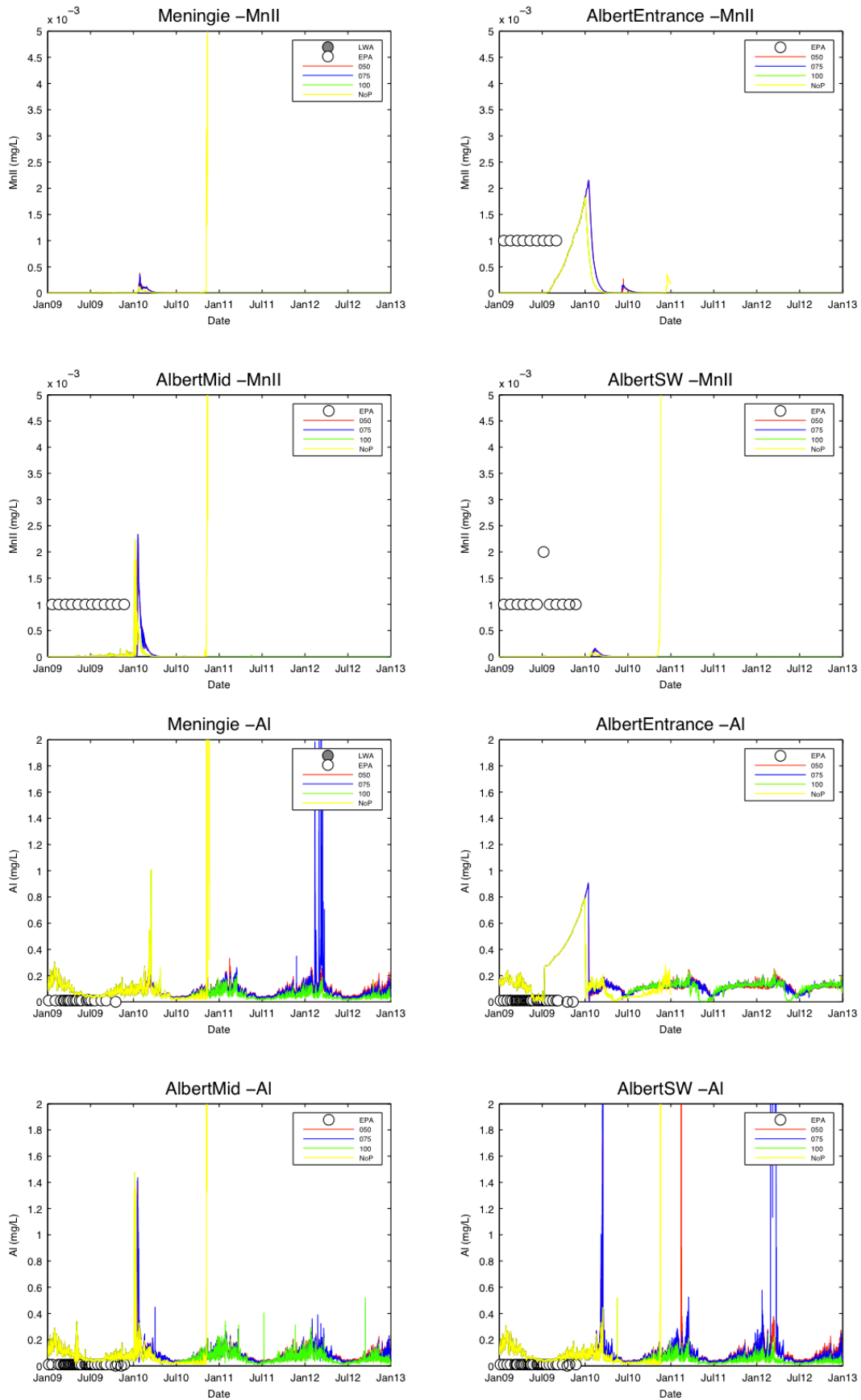
Figure 7.6: Forecast scenarios of modelled (NoP: no continued pumping; 100: stabilisation at -1.0m AHD; 075: stabilisation at -0.75m AHD; 050: stabilisation at -0.5m AHD) dissolved FeII (mg L^{-1}) and calcite (mol L^{-1}) for four stations within Lake Albert.
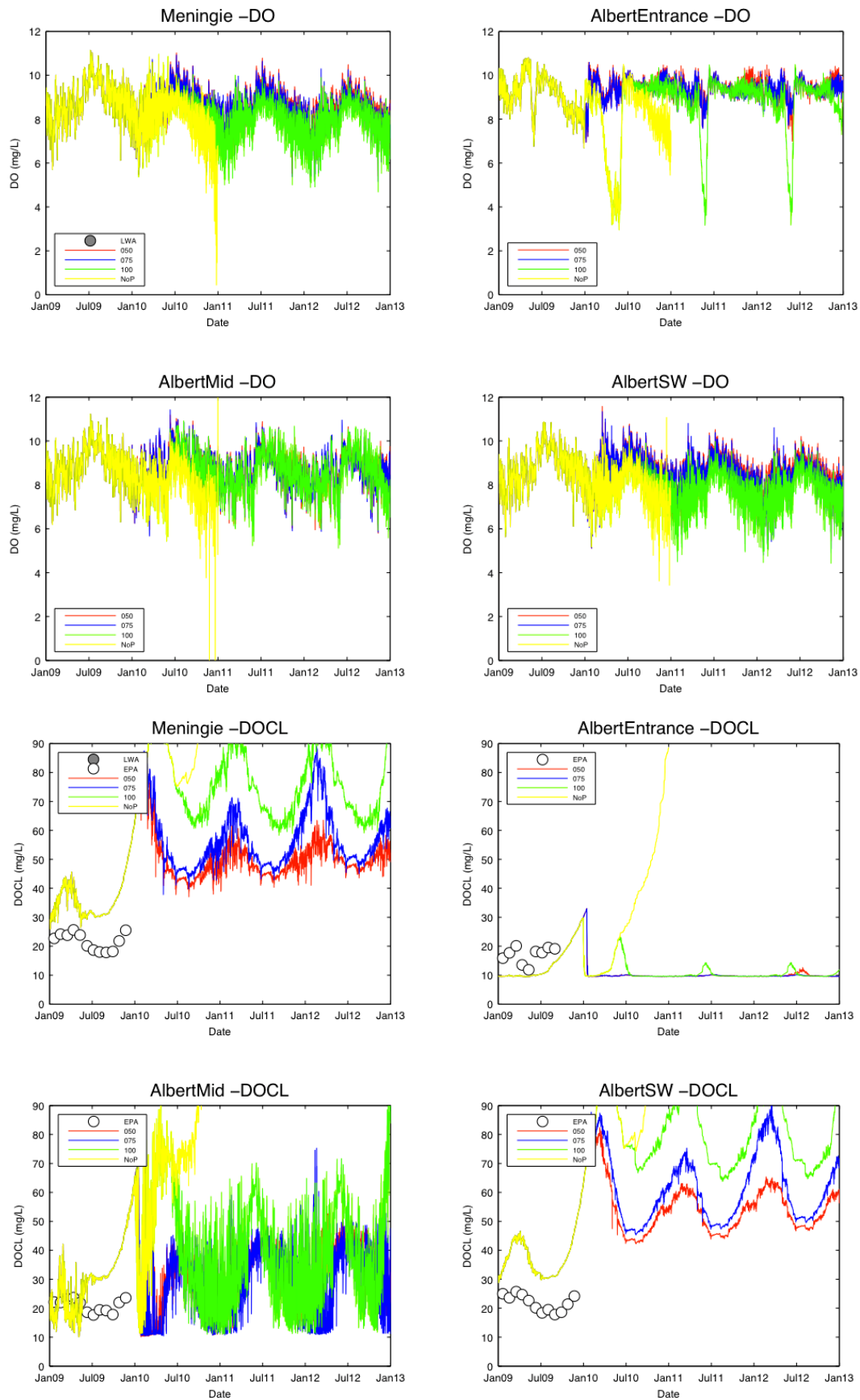
Figure 7.7: Forecast scenarios of modelled (NoP: no continued pumping; 100: stabilisation at -1.0m AHD; 075: stabilisation at -0.75m AHD; 050: stabilisation at -0.5m AHD) dissolved MnII (mg L-1) and dissolved Al (mg L-1) for four stations within Lake Albert.
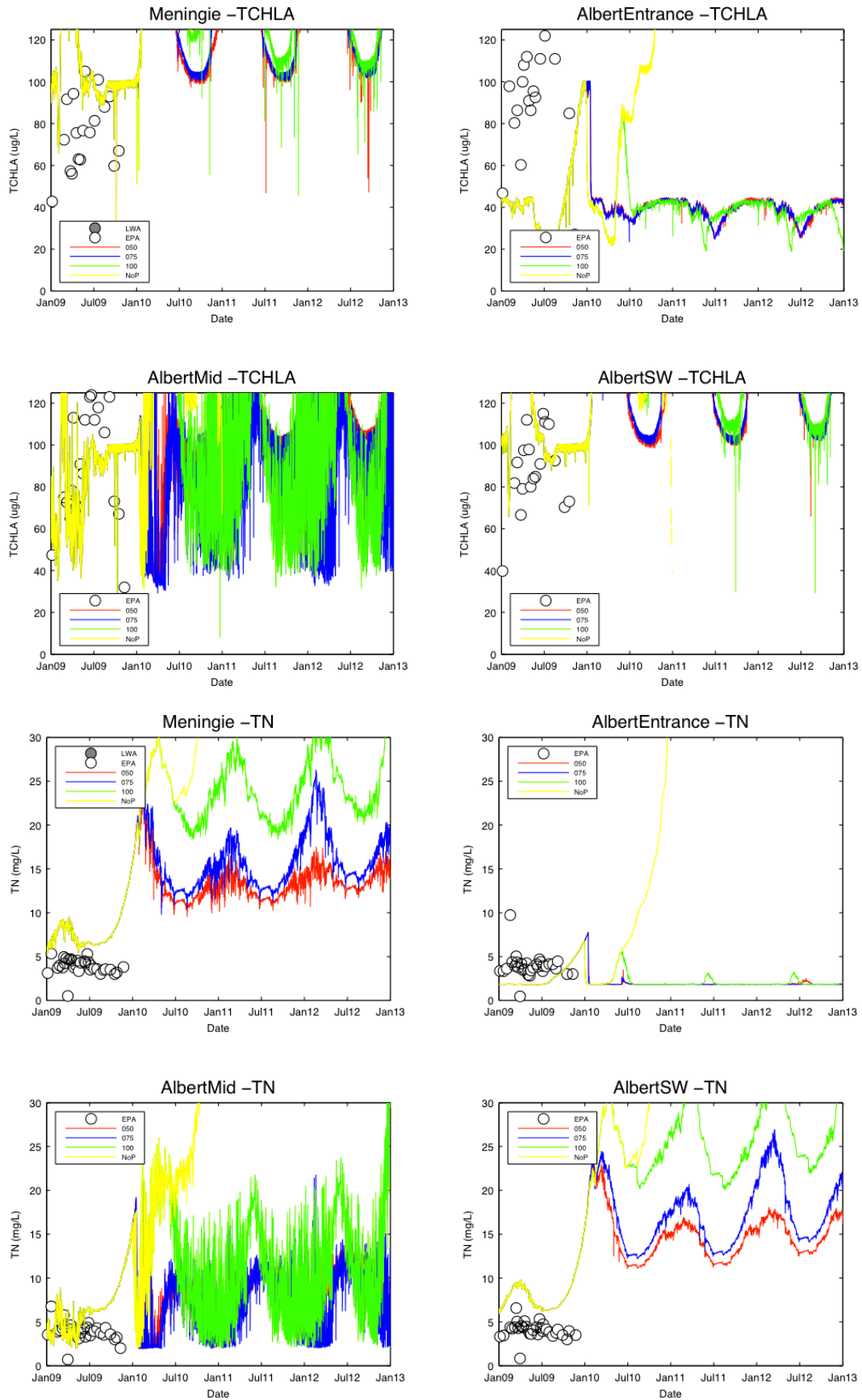
Figure 7.8: Forecast scenarios of modelled (NoP: no continued pumping; 100: stabilisation at -1.0m AHD; 075: stabilisation at -0.75m AHD; 050: stabilisation at -0.5m AHD) DO (mg L^{-1}) and DOC (mg C L^{-1}) for four stations within Lake Albert.

Figure 7.9: Forecast scenarios of modelled (NoP: no continued pumping; 100: stabilisation at -1.0m AHD; 075: stabilisation at -0.75m AHD; 050: stabilisation at -0.5m AHD) total Chlorophyll-a (ug Chla L^{-1}) and TN (mg N L^{-1}) for four stations within Lake Albert.
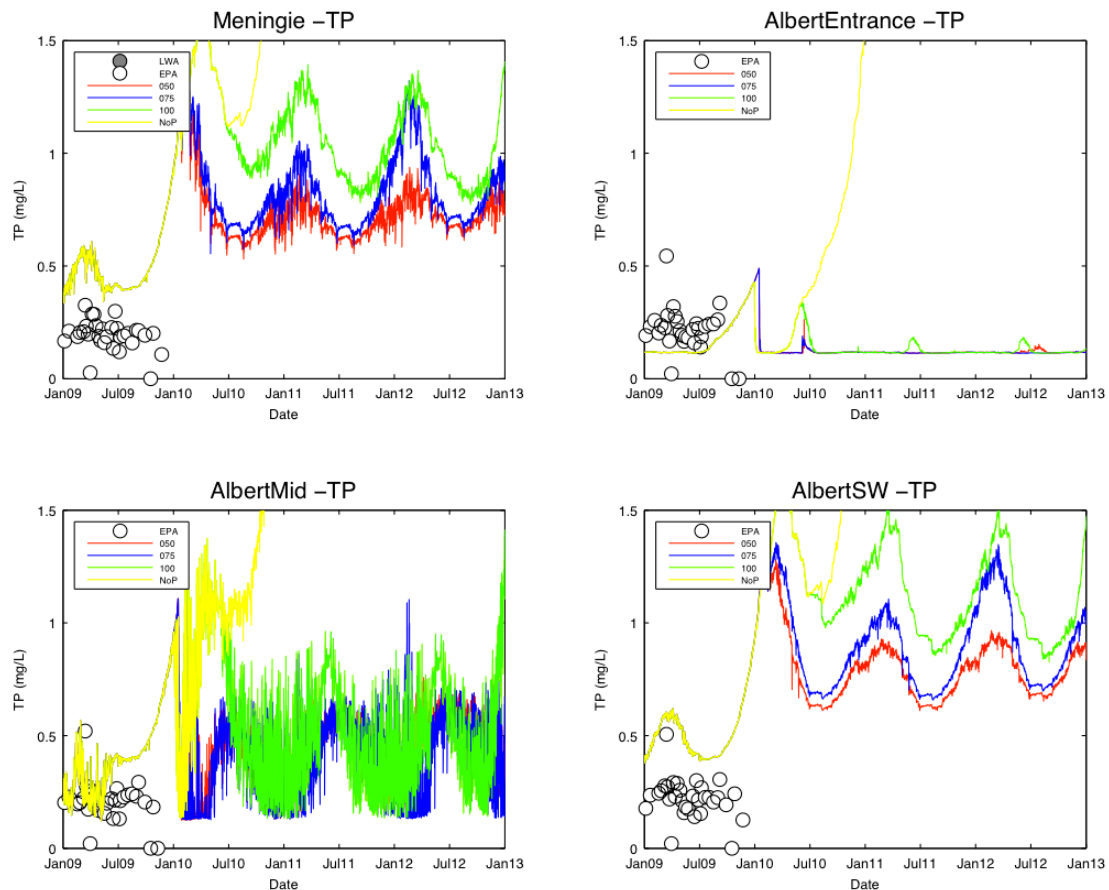
Figure 7.10: Forecast scenarios of modelled (NoP: no continued pumping; 100: stabilisation at -1.0m AHD; 075: stabilisation at -0.75m AHD; 050: stabilisation at -0.5m AHD) TP (mg P L⁻¹) for four stations within Lake Albert.

Lake Albert acid sulfate soil dynamics

Here we aim to gain insights into the processes controlling the acidity dynamics and identify the key sensitive processes by examining spatial variability and integrated process rates. The hydrology output from a cell that started inundated but later became dry is show in Figure 7.11 (-1.0m AHD stabilisation), and highlights the magnitude of the different fluxes over the drying/wetting cycle. Most notably is the magnitude of the overland and throughflow (Q_{se}) that is generated from saturation/infiltration excess generation processes. The chosen cell is clay so the rate of evaporation and drainage is low, and this is reflected in the depth of the drainage that occurs, which is around 0.5m over the 3yr simulation period. However, while only the top 15-20cm of the soil is oxidised, the amount of PASS consumed is considerable given the high initial pyrite content (Figure 7.12).

The spatial plots of pH and soil model output for Lake Albert (Figure 7.13-7.17) show the annual change in the key acidity pools, the key processes controlling acidity mobilisation, and how they vary across the lake. The pH/alkalinity first becomes unstable at the north end of the lake near the opening of the Narrung Narrows to the main body of the lake, and then on the north-western edge near Campbell Park. The southern reach also shows a modest acidity contribution. The lake edge soil properties are patchy due to large variability in soil type (clay or sand) and chemical properties (both PASS and ANC).

The integrated process trends (Figure 7.18) summarise the dynamics as the lake draws down. In particular the rewetting flux in Lake Albert is considerable compared to the other domains simulated. This is because it is a large flat lake and also that the clays are not as conducive to lateral transport and have a higher rewetting acidity flux. Nonetheless the baseflow/seepage component following winter rainfall is substantial, and increases further as the water level declines.
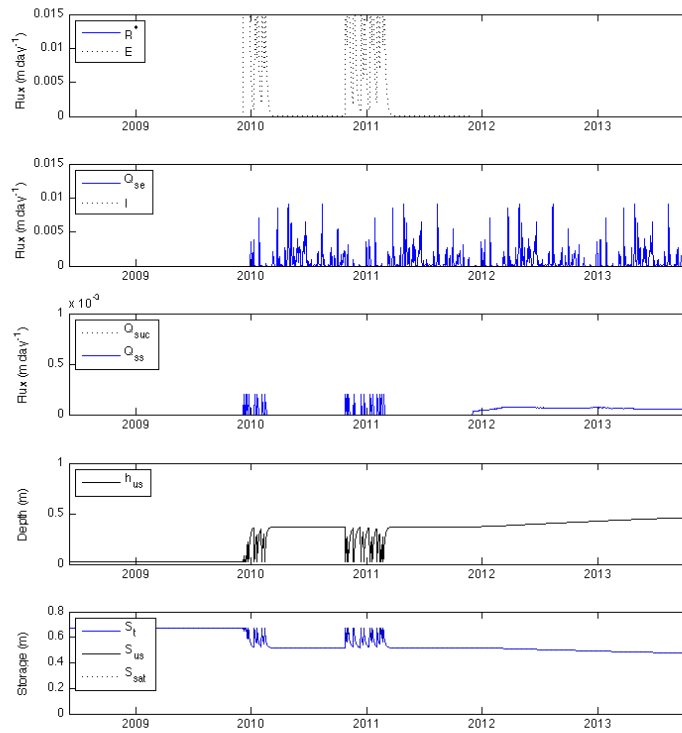
Figure 7.11: Hydrology fluxes in Lake Albert -1.0m AHD stabilisation simulation for a boundary clay cell. Refer to Figure 4.2 for symbol definitions and the hydrological conceptual model.
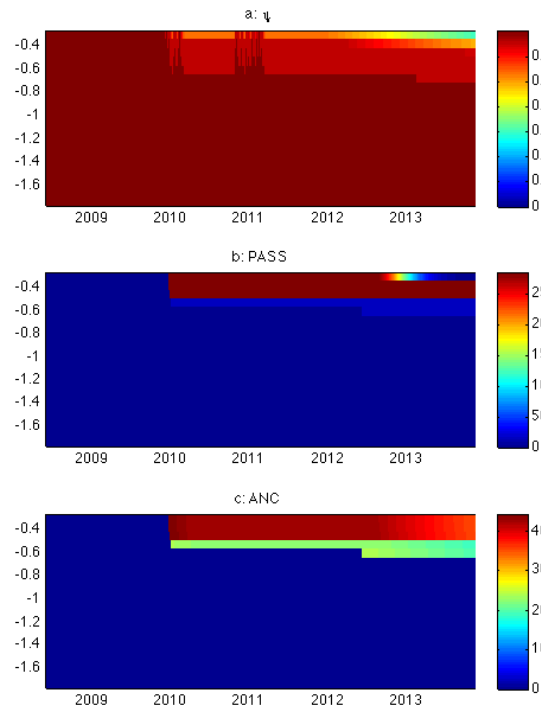

Figure 7.12: Vertical soil profile for a single clay cell on the boundary of Lake Albert during the -1.0m temporary stabilisation showing a) moisture content, b) PASS concentration (mol H+ kg^{-1}) and c) ANC (mol H+ kg^{-1}) evolution.
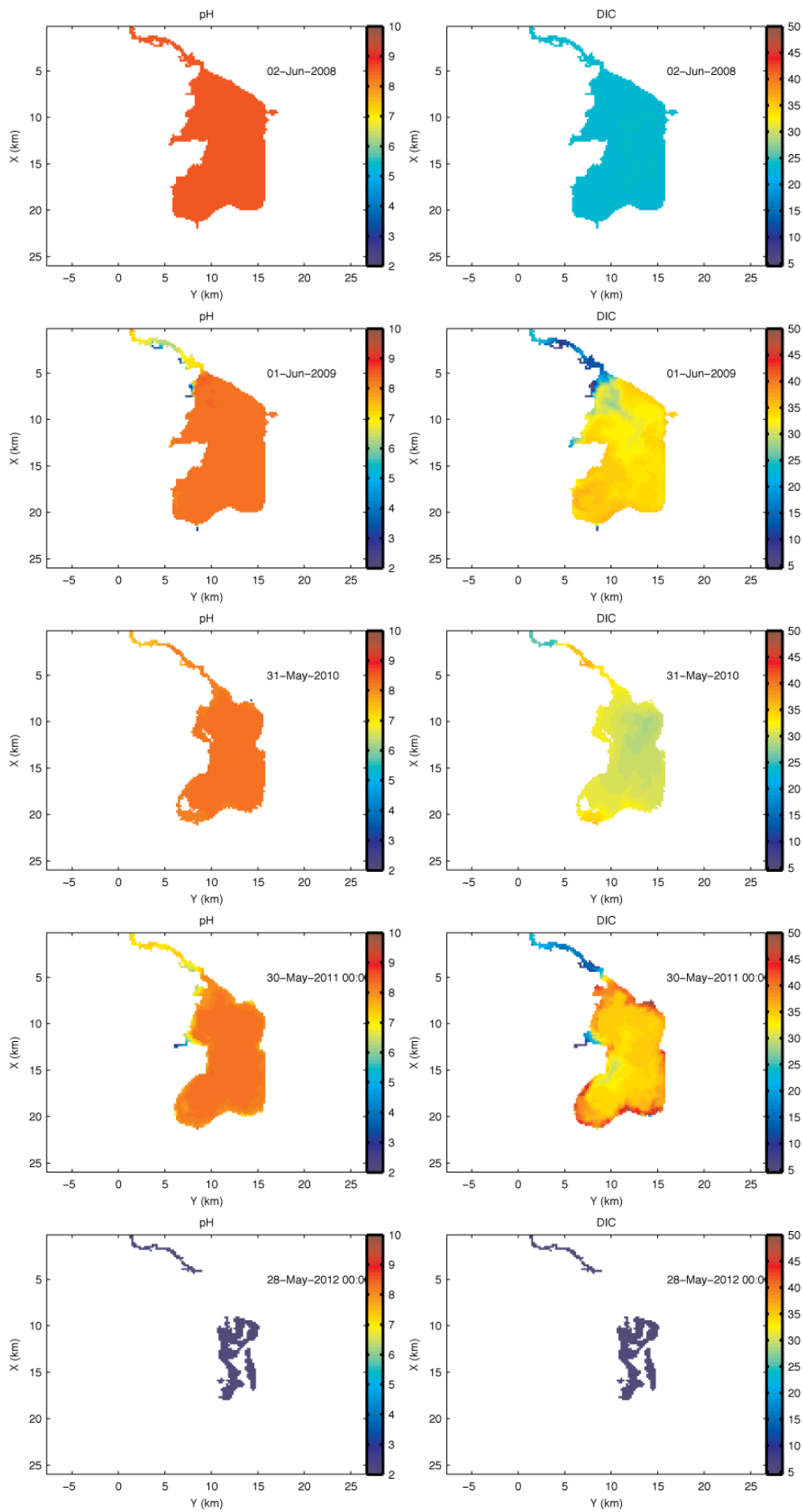
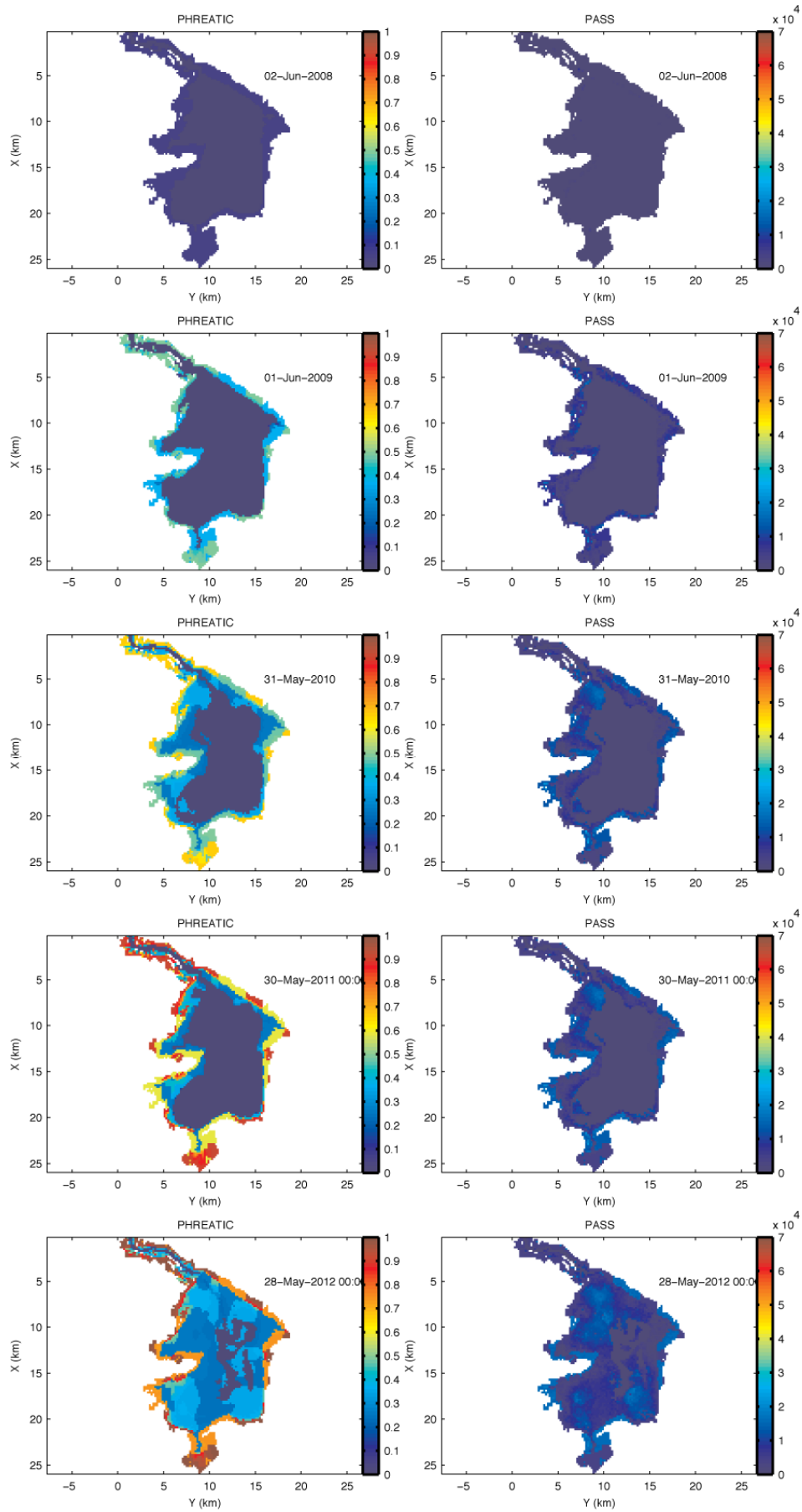Figure 7.13: Plots of pH and DIC (mg C L⁻¹) for Lake Albert at 12-monthly intervals.

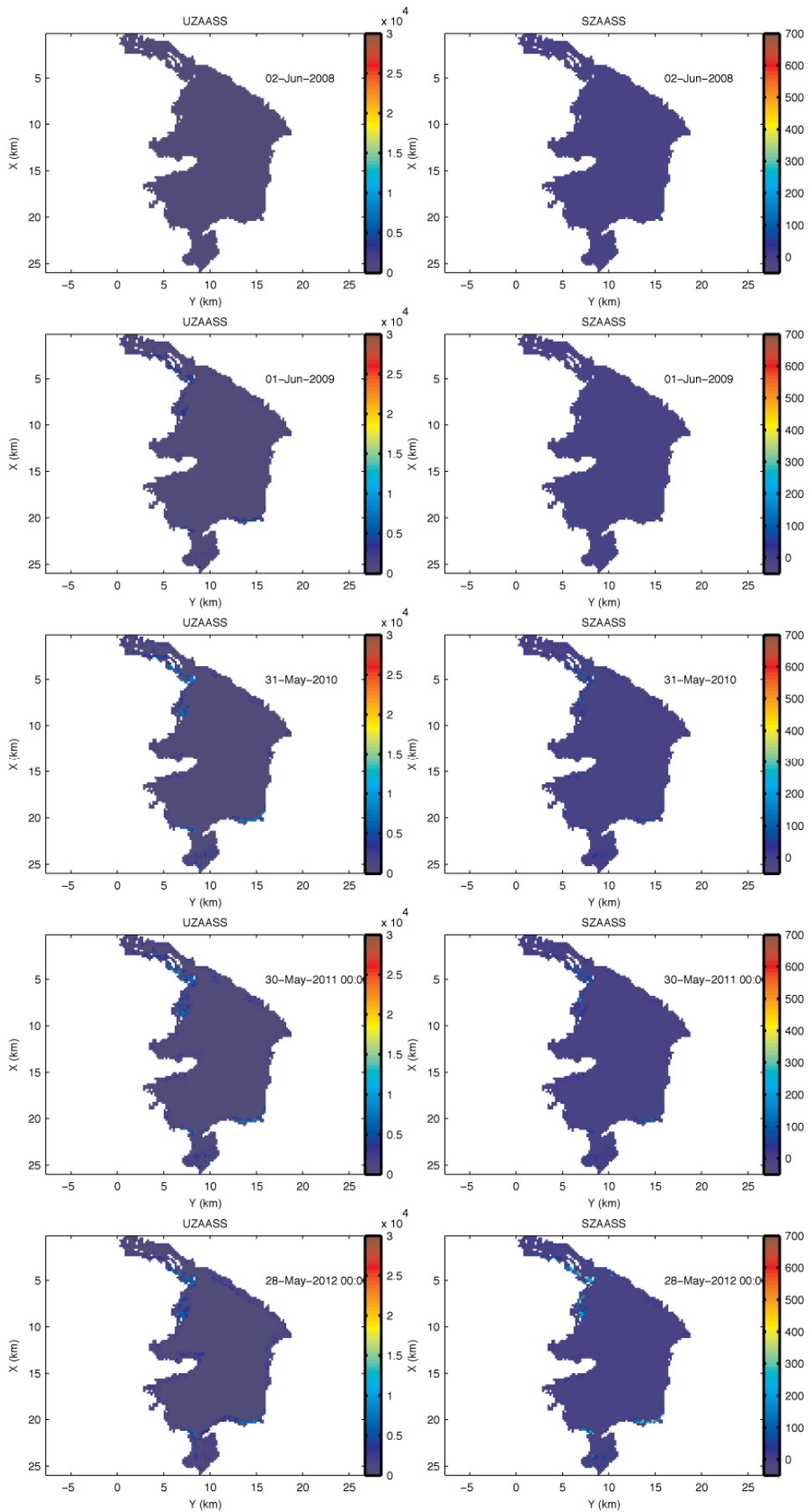**Figure 7.14: Plots of water table depth (PHREATIC, m) and exposed PASS (mol H+ [40000m²]⁻¹) at 12-monthly intervals.**

Figure 7.15: Plots of UZAASS (mol H^+ [40000m^2]$^{-1}$) and SZAASS (mol H^+ [40000m^2]$^{-1}$) at 12-monthly intervals.
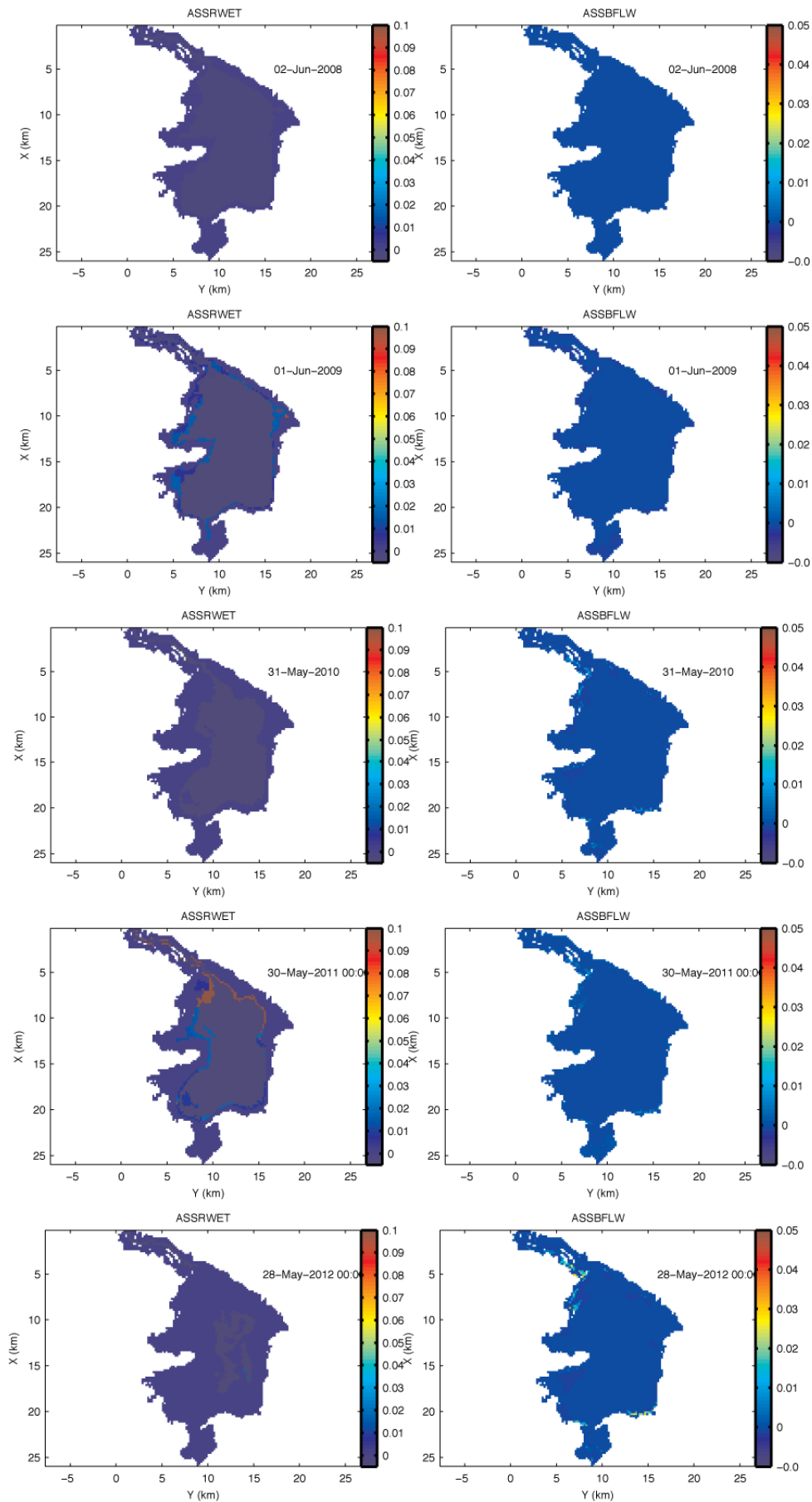
Figure 7.16: Plots of acidity flux rate due ot rewetting (ASSRWET, mol H+ m-2 day-1) and acidity flux rate via baseflow/seepage (ASSBFLW, mol H+ day-1) at 12-monthly intervals.
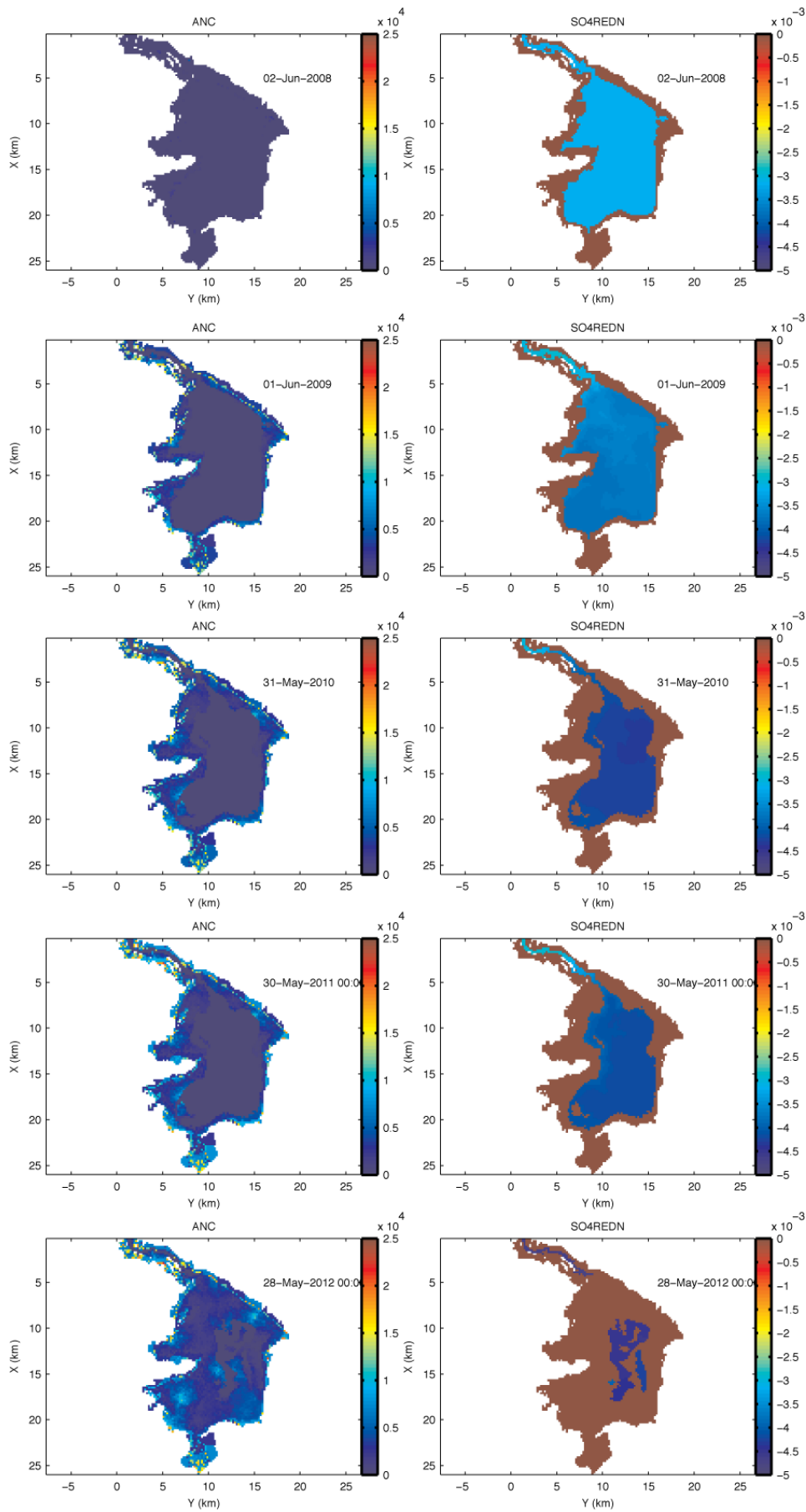
Figure 7.17: Plots of ANC (mol H+ [40000m²]⁻¹) and SO₄ reduction (SO4REDN, x10⁻³ mol H+ m⁻² day⁻¹) at 12-monthly intervals.

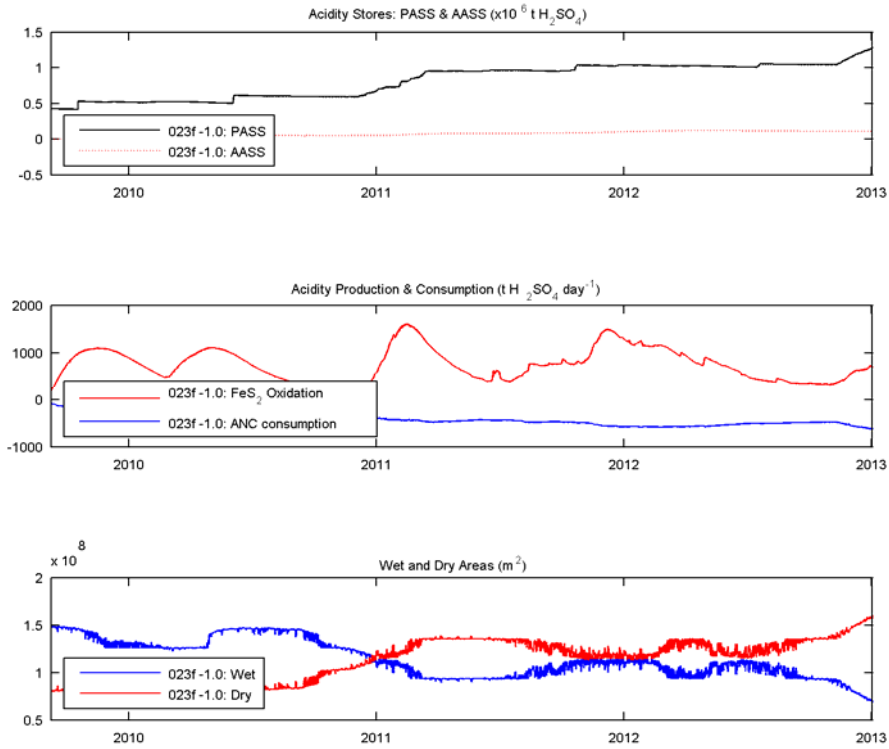**Figure 7.18a: Integrated output from the Lake Albert simulation showing accumulation of exposed PASS and subsequent AASS production and consumption.**
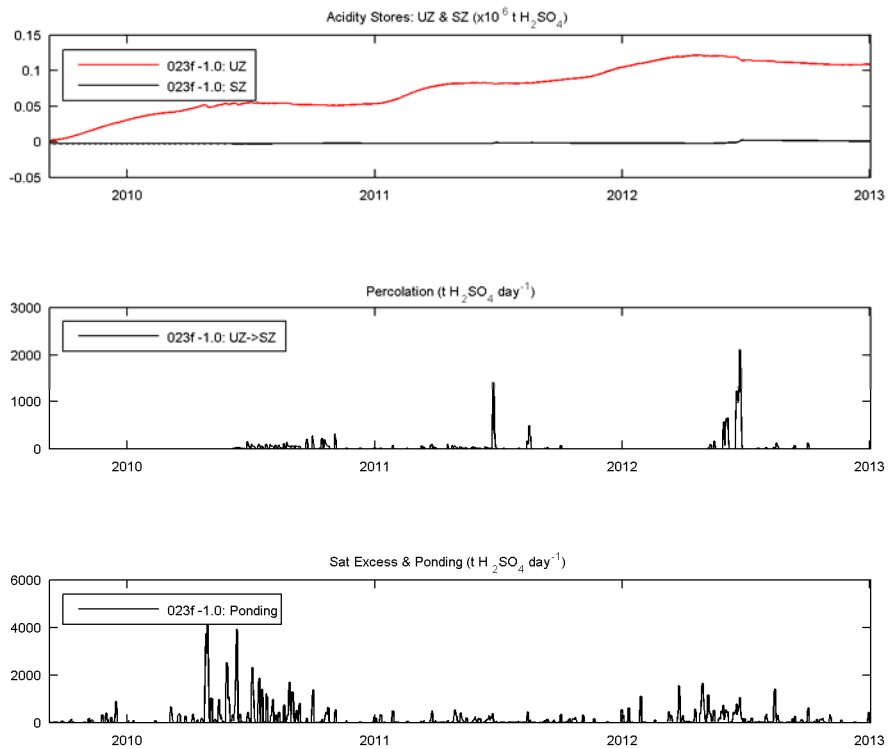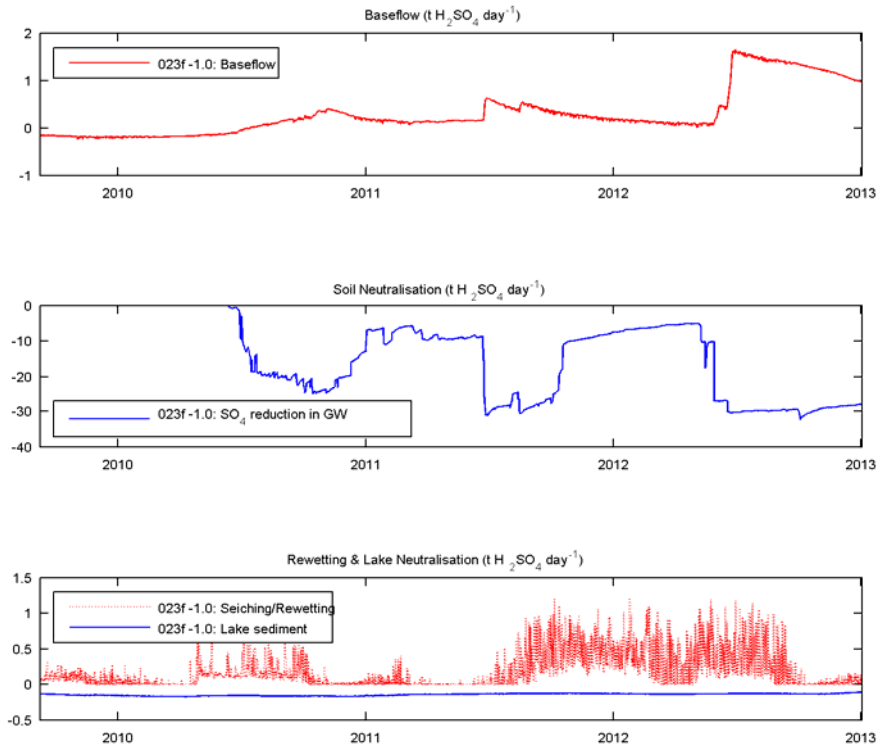

Figure 7.18b: Integrated output from the Lake Albert validation simulation showing the accumulation of acidity in the unsaturated and saturated zone (UZ and SZ respectively), and processes controlling mobilisation.

Figure 7.18c: Integrated output from the Lake Albert simulation showing the baseflow/seepage acidity flux rate, the in-soil neutralisation of acidity by sulfate reduction in the groundwater, and the rewetting flux and in-lake alkalinity flux

To test the sensitivity of the pH predictions to uncertainty in key model parameters identified in Appendix 1, several simulations were conducted with adjusted values of acidity mobilisation fraction (f_{mob}) and ANC neutralisation rate (k_{ANC}). These are denoted '021', '022' and '23f' in Figure 7.19, and have been run for the -1.0 and -0.5 mAHD water-level stabilisation scenarios:

- 021 has high ANC consumption (40% year^{-1}) and a low acidity mobilisable fraction (f_{mob}=0.5);

- 022 has lower ANC consumption (20% year^{-1}) and a low acidity mobilisable fraction (f_{mob}=0.5);

- 23f has lower ANC consumption (20% year^{-1}) and a high acidity mobilisable fraction (f_{mob}=0.75);

The simulations were otherwise configured identically and used 'default' acid sulfate soil and lake model parameters as presented in Table 4.2. From the Currency/Finniss validation, the observed data sat between the 021/022 and 23f ASS sensitivity simulations; this is thus considered to be a reasonable representation of the uncertainty in the predicted alkalinity concentrations. The results indicate a relatively low sensitivity to the ANC neutralisation rate, and a higher sensitivity to the mobilisable fraction (Fig. 7.19). The 23f scenario does create a significant reduction in the alkalinity and a noticeable lowering of the pH compared to the 021/022 simulations. However, the ultimate 'tipping point' is reached around the same time (within 2-3 months of each other), despite the large difference in DIC over the course of the simulations, and this was true for both the -1.0 and -0.5m AHD water-level stabilisation simulations. This highlights that the system is primarily controlled by large rain events that drive mobilisation of substantial amounts of acidity over short time periods, and relatively small differences in the soil available acidity predictions are not overly sensitive in determining the overall outcome, since a substantial acidity reservoir exists.

Annual average budgets of key acidity fluxes and stores of acidity were compiled for the years 2010 and 2012 to gain insights to how the dominant drivers of the acidification process change over time (Figure 7.20) and bearing in mind the different water levels at these times. These sums indicate that the amount of available acidity increases by more than double over this period (these sums assume stabilisation at -1.0mAHD until 2012) and that there is substantial transport of available acidity to the water; in 2010 this is over 30% of the oxidised acidity. In 2012 this reduces to ~18%, however, by this time the store of acidity available for mobilisation is significantly greater. Diffusive fluxes from rewetting and seiching remain small during the drawdown.
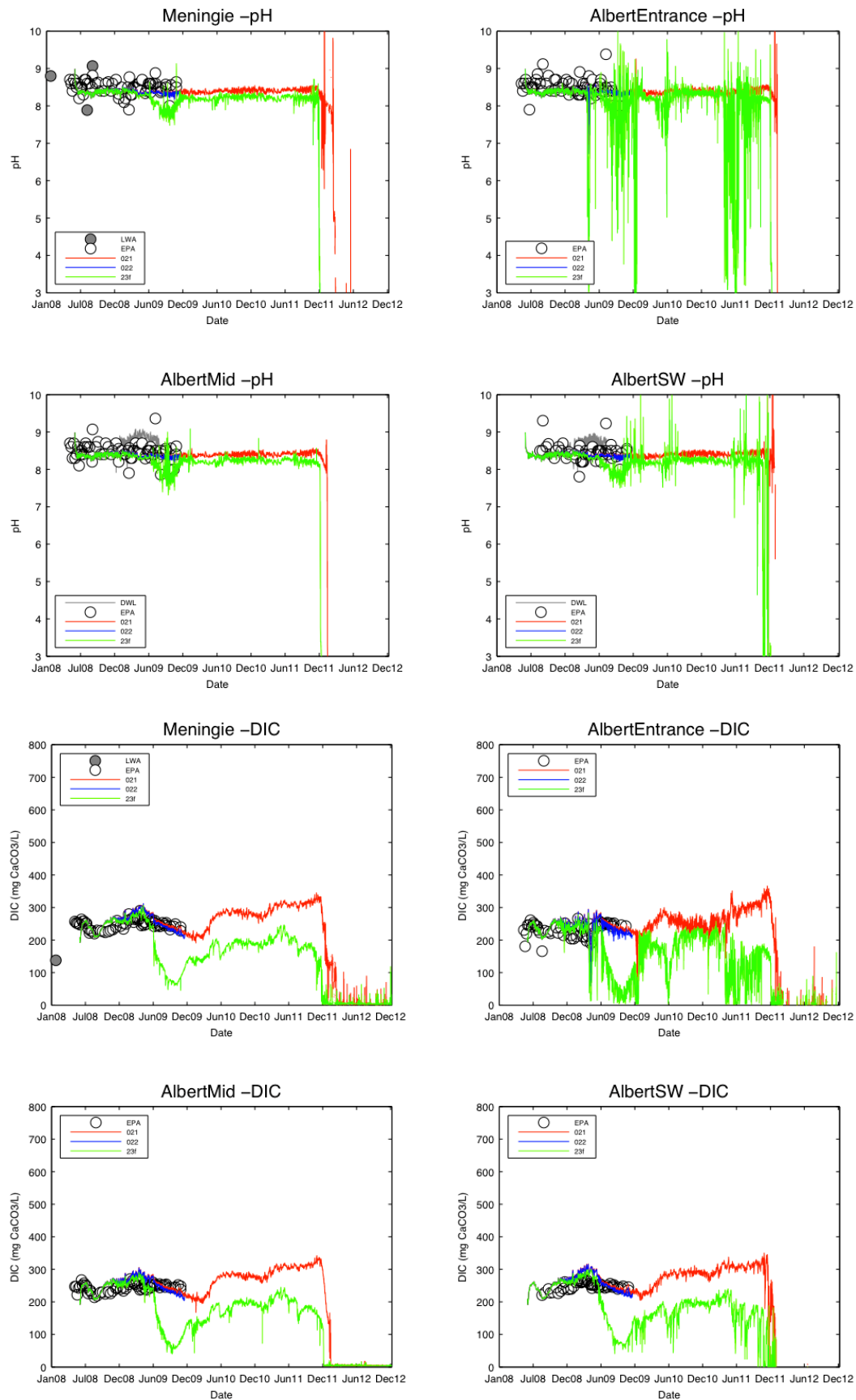
Figure 7.19a: Comparison of Lake Albert pH (top) and DIC (bottom) for three simulations for the -1.0m AHD stabilisation scenario testing sensitivity to the acid neutralisation and mobilisation rates.
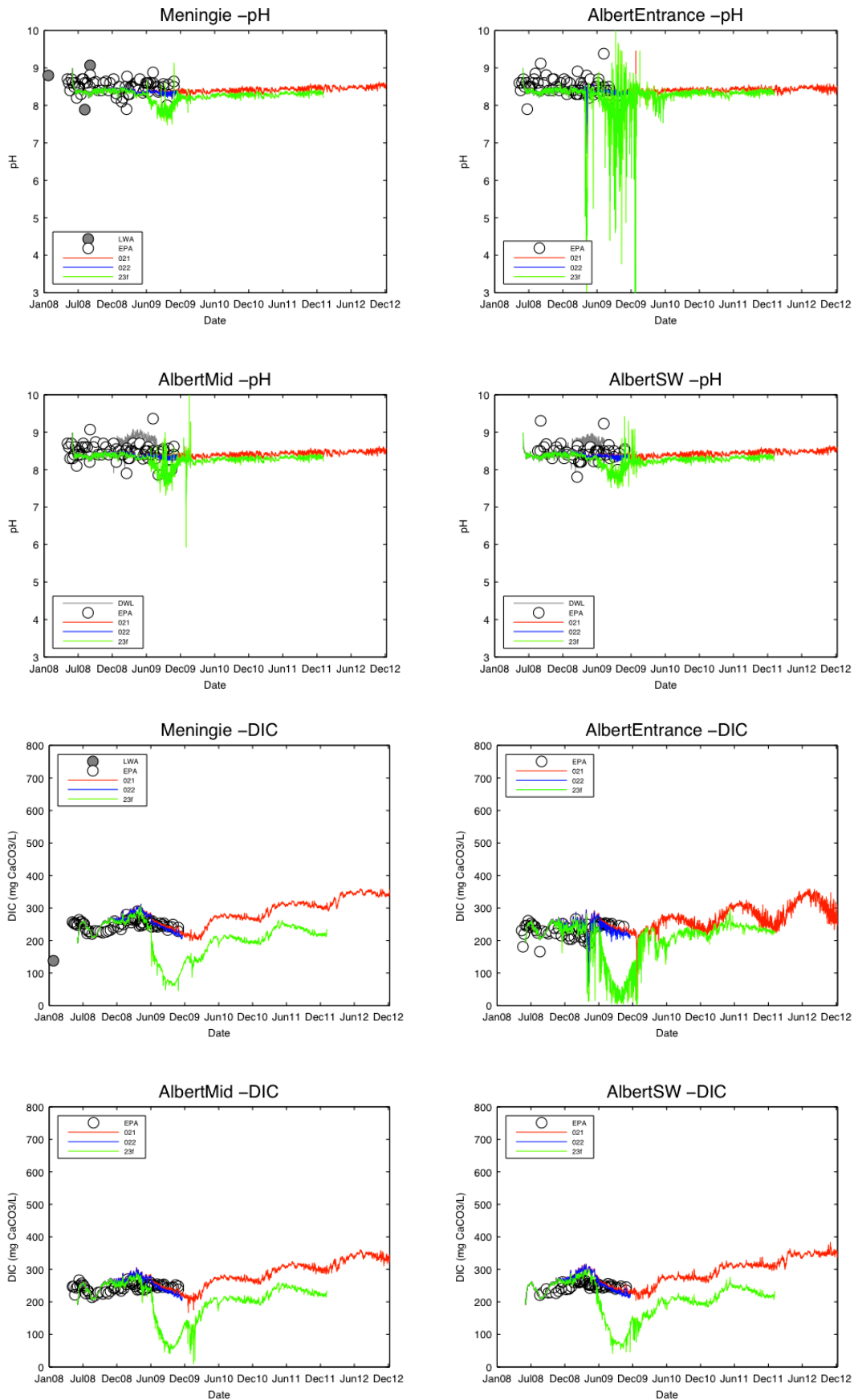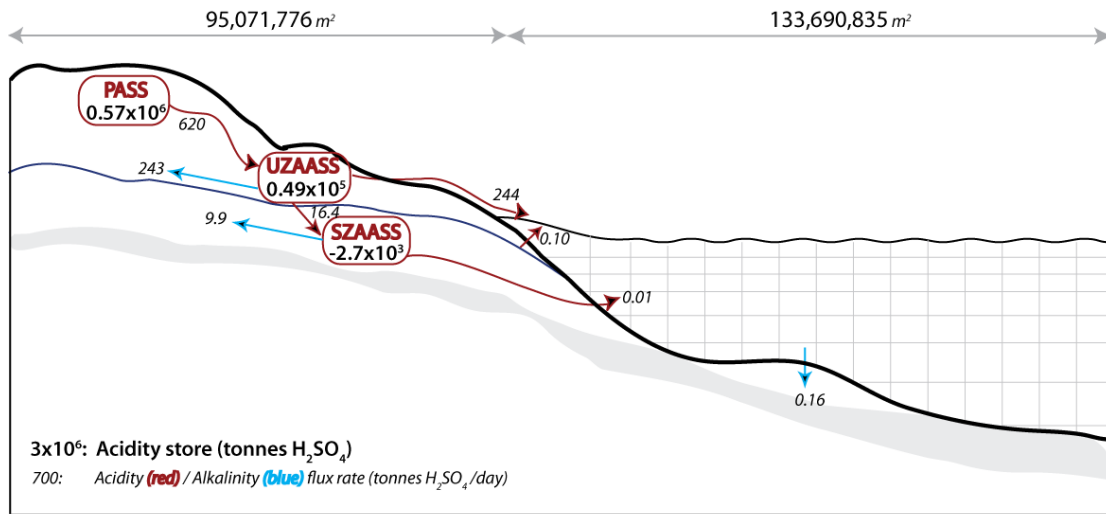
Figure 7.19b: Comparison of Lake Albert pH (top) and DIC (bottom) for three simulations for the -0.5m AHD stabilisation scenario testing sensitivity to the acid neutralisation and mobilisation rates.

2010

95,071,776 m^2 133,690,835 m^2

PASS
0.57x10^6
620

UZAASS
0.49x10^5
243
244
16.4
9.9
SZAASS
-2.7x10^3
0.10
0.01
0.16

3x10^6: **Acidity store (tonnes H$_2$SO$_4$)**
700: *Acidity (red) / Alkalinity (blue) flux rate (tonnes H$_2$SO$_4$/day)*

2012

129,551,522 m^2 99,207,559 m^2

PASS
1.05x10^6
682

UZAASS
1.13x10^5
537
125
42
20
SZAASS
-0.2x10^3
0.28
0.77
0.13

3x10^6: **Acidity store (tonnes H$_2$SO$_4$)**
700: *Acidity (red) / Alkalinity (blue) flux rate (tonnes H$_2$SO$_4$/day)*
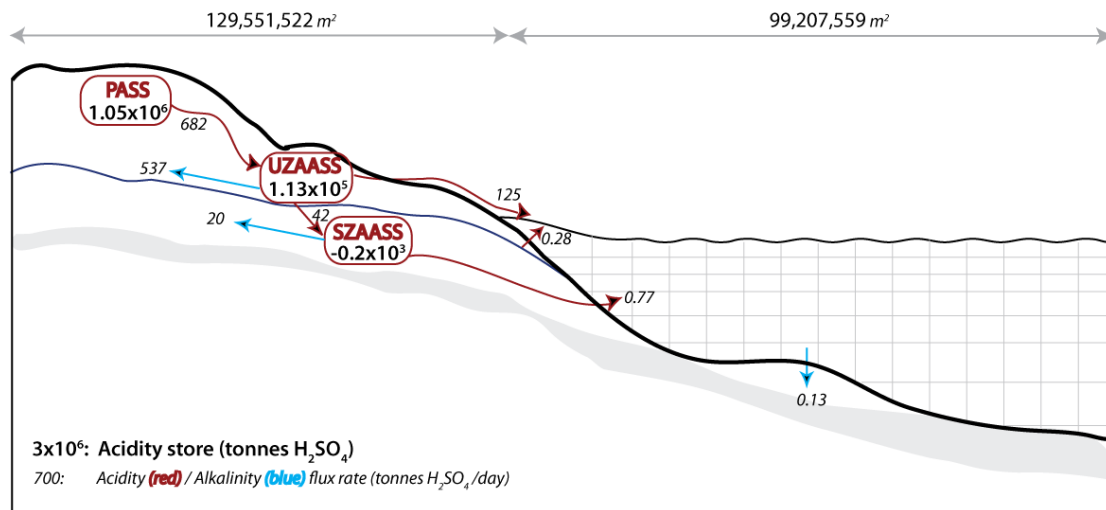
Figure 7.20: Annual average budgets of acidity stores and fluxes for Lake Albert in 2010 and 2012. Data from the -1.0m stabilisation scenario.